CHAPTER TWENTY

From Reaction Networks to Information Flow—Using Modular Response Analysis to Track Information in Signaling Networks

Pascal Schulthess[*,†] *and* Nils Blüthgen[*,†]

Contents

Abstract

Even if the biochemical details of signaling networks are known, it is often hard to track how information flows through the network. In combination with experimental techniques, modular response analysis has proven useful in analyzing the quantitative information transfer in signal transduction networks. The sensitivity of a target (e.g., transcription factor, protein) to an upstream stimulus (e.g., growth factor) can be determined by a so-called response coefficient. We have used this methodology to analyze how information flows in networks where the details of the mechanisms in the networks are known, but parameters are lacking. Using a Monte Carlo approach, we apply this method to track the routes of information flow. More specifically, we determine whether a given species has no, positive or negative influence on any other species in the network. Surprisingly, one can uniquely determine whether a molecule activates or inhibits another one in more than 99% of the interactions solely from the topology of the reaction network. To exemplify the methodology, we briefly discuss three signaling networks of different complexity: (i) a Wnt

* Institute of Pathology, Charité-Universitätsmedizin Berlin, Charitéplatz 1, Berlin, Germany
† Institute for Theoretical Biology, Humboldt University of Berlin, Invalidenstraße 43, Berlin, Germany

Methods in Enzymology, Volume 500
ISSN 0076-6879, DOI: 10.1016/B978-0-12-385118-5.00020-7

signaling pathway model with 15 species, (ii) a MAPK signaling pathway model with 200 species, and (iii) a large-scale signaling network of the entire cell with over 6000 species.

1. Introduction

Even for very small and seemingly simple motifs that we often find in signal transduction, it is hard to systematically deduce whether one molecule activates or deactivates the other. Take, for example, a phosphorylation event, where the kinase K converts the protein A into an active, phosphorylated form A_p (see Fig. 20.1A). Our intuition tells us that K activates A_p. And indeed, if one analyzes the direct effects among the species, one would say that an increase in K leads to a decrease in A and an increase in A_p (see Fig. 20.1B), thereby K activates A_p. However, a decrease in A would also lead to a decrease in A_p, and therefore K indirectly inhibits A_p (see Fig. 20.1C). Thus, K has both a positive and an indirect negative effect on A_p. Of course, for such simple motifs, one could deduce simple rules on how to determine whether a molecule activates or deactivates the other. In our example, a rule could be to investigate the effect on the product of a reaction only. However, this simple example illustrates that it may become very difficult to extract such rules in larger, complex networks, especially if molecules contain multiple modification sites or form complexes.

Therefore, we decided to use the framework of modular response analysis (MRA, see Kholodenko *et al.*, 1997, 2002) to systematically analyze whether the influence of one molecule on another molecule in the network is positive or negative. Section 2 serves as an introduction to the mathematical theory behind MRA. After giving a short overview of conservation analysis in Section 3, we utilize MRA and conservation analysis in Section 4 to extract information flow from reaction networks with the help of a Monte Carlo approach.

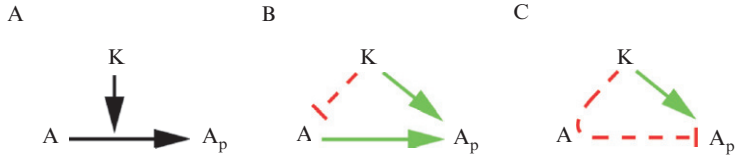

Figure 20.1 Simple reaction network. (A) A kinase K drives the phosphorylation of A to A_p. (B) Direct interactions in the network. (C) Global interactions between K and A_p which are a combination of activation (green solid arrow) and inhibition (red dashed arrow).

2. Modular Response Analysis

MRA has been developed as a framework to analyze interactions between species in hierarchical, information processing networks (Bruggeman *et al.*, 2002; Kholodenko *et al.*, 1997, 2002). It has been proven useful in reverse-engineering of network topologies (Santos *et al.*, 2007), and it has been used to analyze noise in regulatory networks (Bruggeman *et al.*, 2009). MRA is derived from and thus its notations are closely related to metabolic control theory (Heinrich and Rapoport, 1974a,b; Kacser and Burns, 1973). However, as classical metabolic control theory aims at investigating metabolic fluxes, MRA is applicable to systems where there is no flux between different nodes in the network but information transfer.

In the following, we will introduce the mathematical concepts behind MRA exemplified with a small example system, which is described in Fig. 20.2. A substrate S transforms to a product P catalyzed by enzyme E, and P decays back to S. We define the concentration vector $\mathbf{c}(t)$, which collects the concentrations of all species in the network: $\mathbf{c}(t) = [E(t), P(t), S(t)]^{\mathrm{T}}$. There are two fluxes in the network:

$$1 : S \xrightarrow{E} P; \quad 2 : P \rightarrow S; \; \mathrm{E} \leftrightarrow \emptyset \tag{20.1}$$

Assuming mass-action and Michaelis–Menten kinetics, the reaction velocities are then given by:

$$\mathbf{v}(\mathbf{c}(t)) = \begin{bmatrix} v_1(\mathbf{c}(t)) \\ v_2(\mathbf{c}(t)) \\ v_3(\mathbf{c}(t)) \end{bmatrix} = \begin{bmatrix} \dfrac{k_1 E(t) S(t)}{K_{\mathrm{M}} + S(t)} \\ k_2 P(t) \\ k_{+3} - k_{-3} E(t) \end{bmatrix}. \tag{20.2}$$

From the reactions in Eq. (20.1), the stoichiometric matrix $\mathbf{N}$ can be constructed as

$$\mathbf{N} = \begin{bmatrix} 0 & 0 & 1 \\ 1 & -1 & 0 \\ -1 & 1 & 0 \end{bmatrix}, \tag{20.3}$$

where each row refers to the corresponding species in $\mathbf{c}(t)$, and each column describes the corresponding reaction rate in $\mathbf{v}(\mathbf{c}(t))$. One can then describe the dynamics of the concentrations in the system with the following differential equation:

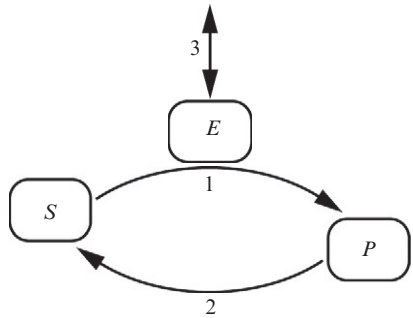

Figure 20.2 Example network. The transformation of substrate S to product P is catalyzed by enzyme E. P then decays to S. Enzyme E is also produced and can decay. Reactions 1 and 2 are irreversible, while reaction 3 is reversible.

$$\frac{\mathrm{d}}{\mathrm{d}t}\mathbf{c}(t) = \mathbf{N}\mathbf{v}(\mathbf{c}(t)) = \mathbf{f}(\mathbf{c}(t)), \tag{20.4}$$

with $\mathbf{c} \in \mathbb{R}^m$, $\mathbf{N} \in \mathbb{R}^{m\times n}$, and $\mathbf{v} \in \mathbb{R}^n$. One property, the so-called unscaled elasticity coefficient, is of particular importance for MRA. The elasticity coefficient characterizes the sensitivity of a reaction rate to perturbations in a species' concentration. Therefore, it provides a measure of the change in a reaction rate in response to a change in a species' concentration. Negative elasticity values represent inhibitory effects of a species on the reaction rate, while positive elasticity values denote activating effects.

For a whole reaction network, this can be expressed by the elasticity coefficient matrix $\boldsymbol{\epsilon} \in \mathbb{R}^{n\times m}$ at steady state $\bar{\mathbf{c}}$. It is formally defined as the partial derivative of $\mathbf{v}(\mathbf{c}(t))$ with respect to $\mathbf{c}(t)$ such that

$$\boldsymbol{\epsilon} = \frac{\partial \mathbf{v}(\mathbf{c}(t))}{\partial \mathbf{c}(t)}\bigg|_{\bar{\mathbf{c}}} = \frac{\partial \bar{\mathbf{v}}}{\partial \bar{\mathbf{c}}}. \tag{20.5}$$

For the example network of Eqs. (20.1)–(20.3), the unscaled elasticity coefficient matrix evaluated at steady state reads:

$$\boldsymbol{\epsilon} = \begin{bmatrix} \dfrac{k_1\bar{S}}{K_\mathrm{M}+\bar{S}} & 0 & \dfrac{k_1 K_\mathrm{M}\bar{E}}{(K_\mathrm{M}+\bar{S})^2} \\ 0 & k_2 & 0 \\ -k_{-3} & 0 & 0 \end{bmatrix}. \tag{20.6}$$

An effect of a species on a reaction has, in turn, effects on the rate by which species change. These effects are captured by the Jacobian matrix $\mathbf{J} \in \mathbb{R}^{m\times m}$,

which is the linearization of the underlying dynamical system. It can be calculated from the stoichiometric matrix and the elasticity matrix:

$$\mathbf{J} = \frac{\partial \mathbf{f}(\mathbf{c}(t))}{\partial \mathbf{c}(t)} = \frac{\partial(\mathbf{N}\mathbf{v}(\mathbf{c}(t)))}{\partial \mathbf{c}(t)} = \mathbf{N}\frac{\partial \mathbf{v}(\mathbf{c}(t))}{\partial \mathbf{c}(t)} = \mathbf{N}\boldsymbol{\epsilon}. \tag{20.7}$$

For our example system, the Jacobian matrix reads:

$$\mathbf{J} = \begin{bmatrix} -k_{-3} & 0 & 0 \\ \dfrac{k_1\bar{S}}{K_M+\bar{S}} & -k_2 & \dfrac{k_1 K_M \bar{E}}{(K_M+\bar{S})^2} \\ -\dfrac{k_1\bar{S}}{K_M+\bar{S}} & k_2 & -\dfrac{k_1 K_M \bar{E}}{(K_M+\bar{S})^2} \end{bmatrix}. \tag{20.8}$$

The entries of the Jacobian can be used to determine whether one node activates or inhibits another node. If an entry $\mathbf{J}_{(k,l)}$ of the matrix is positive, then an increase in node l increases the rate by which node k changes. Consequently, node k influences node l positively.

In order to quantify the strength of the interaction, MRA then defines a so-called local response matrix $\mathbf{r} \in \mathbb{R}^{m\times m}$, which can be interpreted as a normalization of the Jacobian matrix. This matrix can be calculated by dividing the rows of the Jacobian matrix by its diagonal elements:

$$\mathbf{r} = -(\operatorname{diag}(\mathbf{J}))^{-1}\mathbf{J}. \tag{20.9}$$

An entry of this matrix quantifies how a concentration in steady state changes when one perturbs the value of one concentration while others remain constant. As for the Jacobian matrix, a nonzero entry implies that there is a direct link between the corresponding species. Positive and negative entries imply activation and inhibition, respectively. Therefore, the structure of the local response matrix describes the direct interactions between species.

However, if all variables are allowed to change, not only direct interactions but also indirect interactions, that is, interactions over several intermediates, come into play. These influences are given by the global response matrix $\mathbf{R} \in \mathbb{R}^{m\times m}$. Interestingly, this global response matrix can be calculated simply by inversion of the local response matrix:

$$\mathbf{R} = -\mathbf{r}^{-1}. \tag{20.10}$$

The influences between species can be categorized into three different cases. First, species k is inactivated by species l if the (k,l)-th entry is less than zero.

Second, species k activates species l if the (k,l)-th entry is greater than zero. And third, there is no influence from species l to species k if the (k, l)th entry is zero.

For our small example system, the local response matrix reads:

$$\mathbf{r} = \begin{bmatrix} -1 & 0 & 0 \\ \dfrac{k_1\bar{S}}{k_2(K_M+\bar{S})} & -1 & \dfrac{k_1 K_M \bar{E}}{k_2(K_M+\bar{S})^2} \\ -\dfrac{(K_M+\bar{S})\bar{S}}{K_M\bar{E}} & \dfrac{k_2(K_M+\bar{S})^2}{k_1 K_M \bar{E}} & -1 \end{bmatrix}. \tag{20.11}$$

In this example, we immediately see one problem of the approach: The matrix $\mathbf{r}$ has linearly dependent columns (2nd and 3rd column), that is, its determinant is 0. Therefore, an inverse of $\mathbf{r}$ does not exist, and one cannot calculate the global response matrix. The reason for the linear dependence between columns is that there exist conserved moieties, that is, that linear combinations of concentrations remain constant in the system. In our example, the sum of the concentrations of S and P will remain constant.

3. Conservation Analysis

In order to calculate the global response matrix, one needs to reduce the system to variables that are independent. There exists a manifold of algorithms to systematically reduce the system; readers are referred, for example, to Reder (1988) and Vallabhajosyula *et al.* (2006). Once we identified the conserved moieties, we can reorder the species such that the first species (e.g., E and P in the case of the example system) are linearly independent species and the remaining ones are at the end of the vector (e.g., S). Note that there are typically many choices of which species one can use as independent variables. (One could, e.g., also use E and S as independent species.) After reordering the species, one needs to reorder the stoichiometric matrix $\mathbf{N}$ accordingly, which will then decompose into:

$$\mathbf{N} = \begin{bmatrix} \mathbf{N_R} \\ \mathbf{N_0} \end{bmatrix}, \tag{20.12}$$

where $\mathbf{N_R} \in \mathbb{R}^{m_0 \times n}$ has linearly independent rows. Note that the number of rows m_0 of $\mathbf{N_R}$ equals the rank of the stoichiometric matrix $\mathbf{N}$. Further, from conservation analysis, one obtains a link matrix $\mathbf{\Lambda} \in \mathbb{R}^{m \times m_0}$ that relates the stoichiometric matrix of the full system and the one of the reduced system by

$$\mathbf{N} = \mathbf{\Lambda}\mathbf{N}_\mathbf{R}. \tag{20.13}$$

Along with this relationship, we can now reformulate Eq. (20.7) such that

$$\mathbf{J} = \mathbf{\Lambda}\mathbf{N}_\mathbf{R}\boldsymbol{\epsilon}, \tag{20.14}$$

from which the Jacobian matrix for the reduced system results:

$$\mathbf{J}_\mathbf{R} = \mathbf{N}_\mathbf{R}\boldsymbol{\epsilon}\mathbf{\Lambda}. \tag{20.15}$$

For our example system, the matrices $\mathbf{\Lambda}$, $\mathbf{N}_\mathbf{R}$, and $\mathbf{J}_\mathbf{R}$ would read:

$$\mathbf{\Lambda} = \begin{bmatrix} 1 & 0 \\ 0 & 1 \\ 0 & -1 \end{bmatrix}, \quad \mathbf{N}_\mathbf{R} = \begin{bmatrix} 0 & 0 & 1 \\ 1 & -1 & 0 \end{bmatrix}, \tag{20.16}$$

and

$$\mathbf{J}_\mathbf{R} = \begin{bmatrix} -k_{-3} & 0 \\ \dfrac{k_1\bar{S}}{K_\mathrm{M}+\bar{S}} & -\dfrac{k_1 K_\mathrm{M}\bar{E}}{(K_\mathrm{M}+\bar{S})^2} - k_2 \end{bmatrix}. \tag{20.17}$$

The local response matrix of the reduced system $\mathbf{r}_\mathbf{R}$ can now be determined by normalization with the help of Eq. (20.9):

$$\mathbf{r}_\mathbf{R} = \begin{bmatrix} -1 & 0 \\ \dfrac{k_1(K_\mathrm{M}+\bar{S})\bar{S}}{k_1 K_\mathrm{M}\bar{E} + k_2(K_\mathrm{M}+\bar{S})^2} & -1 \end{bmatrix}. \tag{20.18}$$

This matrix can be inverted to gain the global response matrix of the reduced system

$$\mathbf{R}_\mathbf{R} = \begin{bmatrix} 1 & 0 \\ \dfrac{k_1(K_\mathrm{M}+\bar{S})\bar{S}}{k_1 K_\mathrm{M}\bar{E} + k_2(K_\mathrm{M}+\bar{S})^2} & 1 \end{bmatrix}. \tag{20.19}$$

From this, the interaction diagram in Fig. 20.3 can be deduced. Note that for our small example system, the local and global interactions between the linear independent species E and P are the same when we neglect self-loops, as there are no intermediate species present.

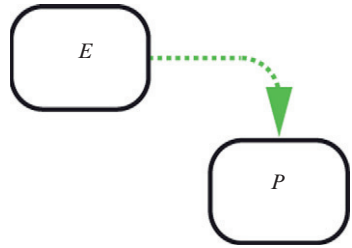

Figure 20.3 Response diagram. Interactions were deduced from the local and the global response matrices of Eqs. (20.18) and (20.19). Activations are marked by a green dashed arrow.

In Section 4, we present a recipe of how to deal with large reaction networks. Further, we perform Monte Carlo computations on the local response matrix and analyze how and to what extend the interactions between species in a system can be determined only from the systems topology.

4. From Reaction Schemes to Influence Networks Using a Monte Carlo Approach

In the following, we exemplify how we can use MRA to extract information flow from reaction networks. Typically, parameters within large-scale networks are unknown or display high uncertainty. Here, we address the question whether we can still deduce qualitatively how information is passed through the network. To do so, we will employ a Monte Carlo approach, where we sample the parameters from a distribution. It was shown that such an approach is very useful when incomplete knowledge about parameters is present (Murabito *et al.*, 2011; Steuer *et al.*, 2006). First, we will reformulate MRA Eq. (20.5) in terms of normalized elasticity coefficients $\tilde{\epsilon}$:

$$\tilde{\epsilon} = \frac{\partial \ln \bar{\mathbf{v}}}{\partial \ln \bar{\mathbf{c}}} = \frac{\bar{\mathbf{c}}}{\bar{\mathbf{v}}} \frac{\partial \bar{\mathbf{v}}}{\partial \bar{\mathbf{c}}} = \frac{\bar{\mathbf{c}}}{\bar{\mathbf{v}}} \epsilon. \tag{20.20}$$

In matrix notation and solving for ϵ, Eq. (20.20) yields

$$\epsilon = \bar{\mathbf{V}} \tilde{\epsilon} \bar{\mathbf{C}}^{-} 1, \tag{20.21}$$

where $\bar{\mathbf{V}} = \mathrm{diag}(\bar{\mathbf{v}})$ and $\bar{\mathbf{C}} = \mathrm{diag}(\bar{\mathbf{c}})$. In Michaelis–Menten-type enzymatic reactions, these normalized elasticity coefficients range typically between zero and one for substrates, zero and minus one for products,

and equal one for enzymes (see also Heinrich and Rapoport, 1974a,b, or any review on metabolic control analysis).
Therefore, the reduced Jacobian is provided by

$$\mathbf{J_R} = \mathbf{N_R}\bar{\mathbf{V}}\widetilde{\boldsymbol{\epsilon}}\bar{\mathbf{C}}^{-1}\boldsymbol{\Lambda}, \tag{20.22}$$

while the local response matrix to investigate reads:

$$\mathbf{r_R} = -(\,\mathrm{diag}(\mathbf{J_R}))^{-1}\mathbf{J_R}. \tag{20.23}$$

These equations are then used to perform Monte Carlo sampling. $\mathbf{N_R}$ and $\boldsymbol{\Lambda}$ are known. Further, the signs of the entries in $\widetilde{\boldsymbol{\epsilon}}$ are known and we decided to sample $\widetilde{\boldsymbol{\epsilon}}$ from a uniform distribution between 0 and 1, and set the sign accordingly. In contrast, the values in the matrices $\bar{\mathbf{V}}$ and $\bar{\mathbf{C}}$ are unknown. Therefore, we chose to sample $\bar{\mathbf{V}}$ and $\bar{\mathbf{C}}$ according to a lognormal distribution with parameters $\mu = 1$ μM and $\sigma = 0.8$ μM (which corresponds to a mean of 3.74 μM and standard deviation of 3.54 μM). For s samples, this results in s different local response matrices $\mathbf{r}^s_\mathbf{R}$.

In a next step, we compare the individual entries $r^s_{R_{k,l}}$ of each sampled system to conclude that (i) an interaction is an inhibition for all s samples if all $r^s_{R_{k,l}} < 0$, (ii) an interaction is an activation for all s samples if all $r^s_{R_{k,l}} > 0$, and (iii) an interaction varies between inhibition and activation when $r^s_{R_{k,l}} \neq 0$ for all s samples and the sign of $r^s_{R_{k,l}}$ changes at least ones in all samples s.

We will now demonstrate the Monte Carlo simulations on the intermediate-scale model of the Wnt pathway. The Wnt signaling plays an important role in carcinogenesis. We use the kinetic model of the canonical Wnt pathway (Fig. 20.4). The model was first derived by Lee *et al.* (2003). If Wnt is not present, the so-called destruction complex consisting of APC, Axin, and GSK3 forms and phosphorylates β-catenin. Phosphorylated β-catenin is a substrate for ubiquitination and thus enters proteolysis. When Wnt is present, it binds to cell surface receptor Frizzled which, in turn, activates disheveled (Dsh). The active form of Dsh inhibits the destruction complex. Then, less destruction complex is present to phosphorylate β-catenin. Subsequently, access β-catenin accumulates and translocates to the nucleus where it regulates genes together with the TCF.

From the conservation analysis, we find that there are four conserved moieties in the model. Therefore, the Wnt model can be reduced from 15 overall species to 11 independent species. The unscaled elasticity coefficient matrix $\boldsymbol{\epsilon}$ can be calculated according to Eq. (20.5). In order to test our approach, we removed the exact kinetic laws, initial conditions, and parameter values defined in the model by Lee *et al.* (2003). We only sustained the signs in $\boldsymbol{\epsilon}$ to preserve the original model structure. We then generated many parameter sets sampled from the aforementioned distributions and

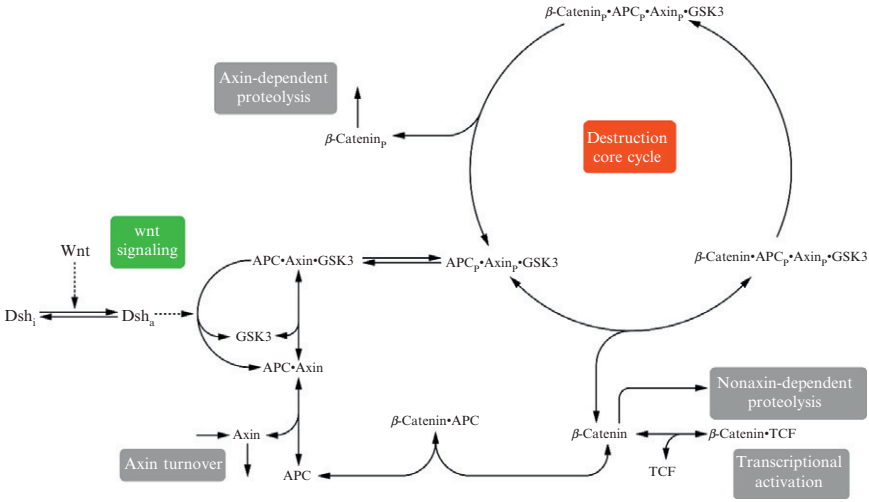

Figure 20.4 Reaction scheme of the Wnt model. Protein complexes are denoted by the names of their components separated by bullets, while phosphorylated, inactive, and active components are marked with a lowercase *p*, a lowercase *i*, or a lowercase *a*, respectively. Single- and double-headed arrows denote irreversible and reversible reactions, respectively. The individual reactions and their role in the Wnt pathway are outlined in the text.

calculated the local response matrix for every sample for each of the parameter sets. When analyzing the effects of the number of Monte Carlo samples, we find that 1000 is a typical number, where even for large-scale networks, larger sample sizes do not provide further information (data not shown). For the reduced Wnt model, we find that the signs of only three local response coefficients change over the different sample sets. All other 26 interactions could be uniquely determined using the Monte Carlo approach to be either activation (12 interactions) or inhibition (14 interactions). We visualized the elements that are positive, negative, or changing between positive and negative over all samples in the interaction diagram of Fig. 20.5. As the diagonal of the local response matrix is minus one by definition, we ignored to visualize the self-inhibitions in the diagram.

Within the sampling process, we can further calculate the global response matrix for every sample in the same way we calculated the local response matrix. The biological most meaningful global interaction is the effect from input (Dsh_i) to output (TCF). The analysis of the corresponding element in $\mathbf{R}_{\mathbf{R}}^{s}$ yields a changing sign for different samples. When we now repeat the whole sampling process a thousand times (i.e., 1000 times 1000 samples), the corresponding element in the global response matrix is positive in 99.3 ± 0.26% of the cases. This result strongly suggests that Dsh_i has an activating effect on TCF.

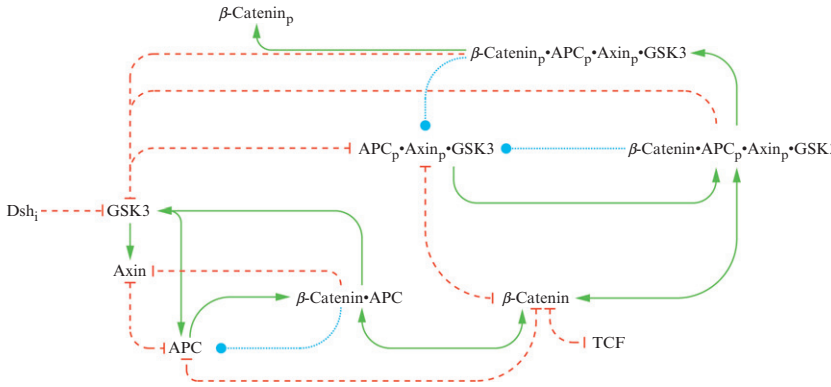

Figure 20.5 Direct interactions in the reduced Wnt model. Protein complexes are denoted by the names of their components separated by bullets, while phosphorylated, inactive, and active components are marked with a lowercase *p*, a lowercase *i*, or a lowercase *a*, respectively. Single-headed arrows describe a directed influence, while double-headed arrows depict a mutual interaction between the connected species. Inhibition and activation are shown with red dashed and green solid arrows, respectively, while blue dotted arrows mask a nondeterminable interaction type.

The high percentage of uniquely determinable local interactions leads to the hypothesis that the knowledge of interaction type and the stoichiometric matrix is sufficient to unveil the directionality of information flow also in larger systems. To test this hypothesis, we applied our approach to larger and very large signal transduction models. As one example, we used an SBML (Bornstein *et al.*, 2008) implementation of the MAPK model by Schoeberl *et al.* (2002) that has 97 species and 148 reactions. Conservation analysis yields five conserved moieties. As another example, we translated the whole signaling part of the Reactome database (Matthews *et al.*, 2009; Vastrik *et al.*, 2007) into a stoichiometric and an elasticity coefficient matrix with 6232 species and 3652 reactions. Conservation analysis shows that about half of the present species are linearly dependent in this large network.

In Fig. 20.6, we compare the four models (e.g., Example, Wnt, MAPK, and Reactome) with respect to the distributions of the signs in the local response matrices over all 1000 samples. What becomes apparent is that even for larger models, the fraction of interactions that change their signs over the different sampling sets are very low. For the MAPK model, there were only about 1.3% of all possible interactions, while the Reactome model yielded a fraction of 0.6‰ of the nonunique interactions. Especially in the Reactome network, the percentage of species that interact directly is obviously very low. Here, also the fraction of unambiguous positive and negative interactions is very low as well (1.5‰ and 1.8‰).

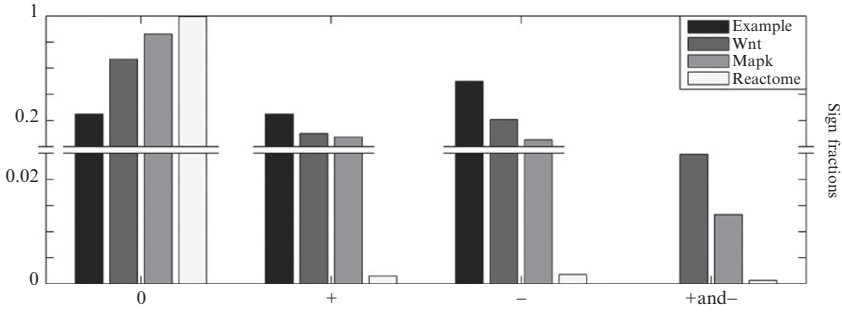

Figure 20.6 **Sign distribution. Fractions of signs in the local response matrix with respect to the number of elements in r. 0, +, and − represent the fraction of elements that are always zero, always positive, and always negative, respectively. The fourth column of bars represents elements that change their sign over different samples.**

In conclusion, our Monte Carlo simulations using modular response and conservation analysis show that the sign of interaction (activation or inhibition) is in most cases already defined through the kinetic scheme of the reaction network and does not require knowledge of the parameters. More than 99% of the signs of the local response matrix could be identified uniquely from the structure of the reaction network. That means, even without knowing the reaction network in detail, the direction and sign of information flow can often be determined.

5. Conclusion

Information flow is the important property of biochemical signaling networks. It determines the effect of a stimulus on the readout of a network. In this chapter, we presented a recipe to tackle this question on a computational and qualitative level. MRA serves as a handy instrument to gain an insight to otherwise hidden network properties. In combination with conservation analysis, we could show that a very high percentage of species interactions could be determined solely from the topology of the network. This method is applicable to molecular reaction systems where not all parameters of kinetic laws are known, especially for large and very large signaling networks.

ACKNOWLEDGMENTS

We thank Bente Kofahl for providing a Mathematica notebook of the Wnt model. We also thank Ralf Steuer for very helpful discussions, and Franziska Witzel for critically reading the chapter. This work was supported by CancerSys (EU FP7) and FORSYS (BMBF).

REFERENCES

Bornstein, B. J., Keating, S. M., Jouraku, A., and Hucka, M. (2008). Libsbml: An Api library for sbml. *Bioinformatics* **24,** 880–881.

Bruggeman, F. J., Westerhoff, H. V., Hoek, J. B., and Kholodenko, B. N. (2002). Modular response analysis of cellular regulatory networks. *J. Theor. Biol.* **218,** 507–520.

Bruggeman, F. J., Bluethgen, N., and Westerhoff, H. V. (2009). Noise management by molecular networks. *PLoS Comput. Biol.* **5,** e1000506.

Heinrich, R., and Rapoport, T. A. (1974a). A linear steady-state treatment of enzymatic chains. General properties, control and effector strength. *Eur. J. Biochem.* **42,** 89–95.

Heinrich, R., and Rapoport, T. A. (1974b). A linear steady-state treatment of enzymatic chains. Critique of the crossover theorem and a general procedure to identify interaction sites with an effector. *Eur. J. Biochem.* **42**(1), 97–105.

Kacser, H., and Burns, J. A. (1973). The control of flux. *Symp. Soc. Exp. Biol.* **27,** 65–104.

Kholodenko, B. N., Hoek, J. B., Westerhoff, H. V., and Brown, G. C. (1997). Quantification of information transfer via cellular signal transduction pathways. *FEBS Lett.* **414,** 430–434.

Kholodenko, B. N., Kiyatkin, A., Bruggeman, F. J., Sontag, E., Westerhoff, H. V., and Hoek, J. B. (2002). Untangling the wires: A strategy to trace functional interactions in signaling and gene networks. *Proc. Natl. Acad. Sci. USA* **99,** 12841–12846.

Lee, E., Salic, A., Krueger, R., Heinrich, R., and Kirschner, M. W. (2003). The roles of apc and axin derived from experimental and theoretical analysis of the Wnt pathway. *PLoS Biol.* **1,** 116–132.

Matthews, L., Gopinath, G., Gillespie, M., Caudy, M., Croft, D., de Bono, B., Garapati, P., Hemish, J., Hermjakob, H., Jassal, B., Kanapin, A., Lewis, S., *et al.* (2009). Reactome knowledgebase of human biological pathways and processes. *Nucleic Acids Res.* **37,** D619–D622.

Murabito, E., Smallbone, K., Swinton, J., Westerhoff, H. V., and Steuer, R. (2011). A probabilistic approach to identify putative drug targets in biochemical networks. *J. R. Soc. Interface* **8,** 880–895.

Reder, C. (1988). Metabolic control theory: A structural approach. *J. Theor. Biol.* **135,** 175–201.

Santos, S. D. M., Verveer, P. J., and Bastiaens, P. I. H. (2007). Growth factor-induced mapk network topology shapes erk response determining. pc-12 cell fate. *Nat. Cell Biol.* **9,** 324–330.

Schoeberl, B., Eichler-Jonsson, E., Gilles, E. D., and Mueller, G. (2002). Computational modeling of the dynamics of the map kinase cascade activated by surface and internalized egf receptors. *Nat. Biotechnol.* **20,** 370–375.

Steuer, R., Gross, T., Selbig, J., and Blasius, B. (2006). Structural kinetic modeling of metabolic networks. *Proc. Natl. Acad. Sci. USA* **103,** 11868–11873.

Vallabhajosyula, R. R., Chickarmane, V., and Sauro, H. M. (2006). Conservation analysis of large biochemical networks. *Bioinformatics* **22,** 346–353.

Vastrik, I., D'Eustachio, P., Schmidt, E., Joshi-Tope, G., Gopinath, G., Croft, D., de Bono, B., Gillespie, M., Jassal, B., Lewis, S., Matthews, L., Wu, G., *et al.* (2007). Reactome: A knowledge base of biologic pathways and processes. *Genome Biol.* **8,** R39.